ELSEVIER

Biomaterials 20 (1999) 1783–1790

Biomaterials

Biodegradable polymeric microcellular foams by modified thermally induced phase separation method

Yoon Sung Nam, Tae Gwan Park*

Department of Biological Sciences, Korea Advanced Institute of Science and Technology, 373-1 Kusong-dong Yusong-gu, Taejon 305-701, South Korea

Received 3 December 1998; accepted 7 April 1999

Abstract

Thermally induced phase separation (TIPS) for the fabrication of porous foams based on various biodegradable polymers of poly(L-lactic acid) and its copolymers with D-lactic acid and/or glycolic acid is presented. Diverse foam morphologies were obtained by systematically changing several parameters involved in the TIPS process, such as polymer type and concentration, coarsening conditions, solvent/nonsolvent composition, and the presence of an additive. The produced foams had microcellular structures with average pore diameters ranging from 1 to 30 μm depending on the process parameters, which were characterized by scanning electron microscopy (SEM) and mercury intrusion porosimetry. Additionally, Pluronic F127 was used as an additive porogen to control the pore geometry and size.

Keywords: Biodegradable polymers; Poly(L-lactic acid); Foams; Tissue engineering; Thermally induced phase separation

1. Introduction

Poly(L-lactic acid) [PLLA] and its copolymers with D-lactic acid and/or glycolic acid have been extensively explored for biodegradable drug delivery carriers and tissue engineering scaffolds due to their superior biocompatibility and versatile processabilities. For tissue engineering scaffolds, a macroporous open cellular structure is often required with pore sizes of 100–300 μm for cell penetration. The most popularly used polymer scaffold in soft tissue regeneration is heat-compressed nonwoven fiber mesh of polyglycolic acid. However, it is not suitable for hard tissue regeneration due to the weak mechanical strength [1,2]. Several other techniques have been developed for the fabrication of porous biodegradable polymers useful for cell transplantation: solvent casting/salt leaching [3,4], phase separation [5,6], emulsion freeze drying [7], and gas foaming [8,9]. These methods generally intend to generate large open porous matrices for penetration and in-growth of bone and cartilage cells. On the other hand, it is often necessary to manufacture microcellular foams with pore diameters ranging from 10 to 100 μm for optimal in-growth of fibroblasts for the tissue regeneration of skin. Concomitantly, achieving sustained release capability of a therapeutic protein through these porous biodegradable matrices is desirable for improving the viability of cells seeded within the matrices [5].

Thermally induced phase separation (TIPS) is currently utilized to fabricate microporous membranes or microcellular foams [10–12]. This technique is based on the principle that a single homogeneous polymer solution made at elevated temperature is converted via the removal of thermal energy to two-phase separated domains composed of a polymer-rich phase and a polymer-lean phase [13–15]. Subsequent freeze-drying of the liquid–liquid phase-separated polymer solution produces microcellular structures as a result of solvent removal. A schematic temperature–composition phase diagram for a binary polymer–solvent system is represented in Fig. 1. It shows the expected variations in polymer foam morphology depending on the final thermodynamic state of the polymer solution to be thermally quenched. According to whether the quenching end point is located in the metastable region between binodal and spinodal curves or in the unstable region below the spinodal curve, two distinctive morphologies can be obtained: (i) a poorly interconnected bead-like structure by a nucleation and growth mechanism or (ii) a well-interconnected open

* Corresponding author. Tel.: +82-42-8692621; fax: +82-42-8692610.

E-mail address: tgpark@sorak.kaist.ac.kr (T.G. Park)

0142-9612/99/$ - see front matter
PII: S0142-9612(99)00073-3

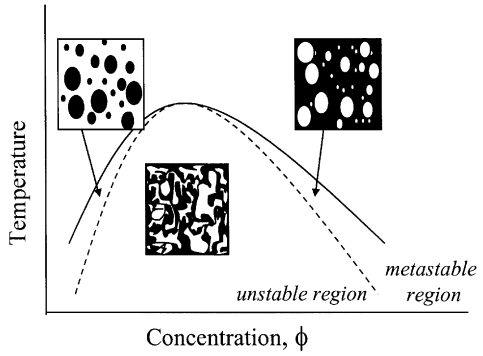

Fig. 1. A schematic representation of a binary phase diagram of a polymer solution showing the expected morphological variations from liquid–liquid-phase separation.

porous structure by a spinodal decomposition mechanism. It is necessary to preferably utilize the spinodal decomposition for the production of open-pore microcellular foams. Pore size distribution and their interconnectivity of the resultant microcellular foams are determined by a delicate balance of various parameters such as polymer concentration, quenching route, quenching depth, solvent/nonsolvent composition, and the presence of additives. Additionally, the effect of ripening and coalescence in the liquid–liquid phase separation plays an important role in determining the final foam morphology via a coarsening process. This effect is induced by differential interfacial tension exerted between the two phase-separated domains. It was demonstrated that the coarsening process results in pore size enlargement primarily via Ostwald ripening, coalescence, or hydrodynamic flow mechanism [16,18]. Thus, the coarsening process should be carefully considered as a kinetic parameter to control the pore morphology of the resultant foams.

In this study, PLLA, poly(D,L-lactic acid) [PDLLA], poly(D,L-lactic-co-glycolic acid [PLGA] were used for the preparation of various microcellular foam structures by adjusting parameters involved in the TIPS process. Pure 1,4-dioxane, a good solvent for the polymer, was used for a solid–liquid phase separation, and water was added as a nonsolvent to induce a liquid–liquid phase separation by lowering the degree of polymer–diluent interaction. The addition of Pluronic surfactant in the TIPS formulation was also examined in order to better control the pore morphology.

2. Materials and methods

2.1. Materials

Poly(L-lactic acid) (PLLA), poly(D,L-lactic acid) (PDLLA), and poly(D,L-lactic-co-glycolic acid, lactide : glycolide ratio 85 : 15) (PLGA) were supplied by Medisorb (Cincinnati, OH). Weight and number average molecular weights were determined by gel permeation chromatography (GPC) as described elsewhere [19]; $M_w = 59{,}000$ and $M_n = 28{,}500$ for PLLA, $M_w = 74{,}500$ and $M_n = 35{,}900$ for PDLLA, and $M_w = 74{,}700$ and $M_n = 46{,}000$ for PLGA. Carbonic anhydrase II (from bovine erythrocytes, cat. # C-2522) and Coomassie Blue R-250 were obtained from Sigma and Pluronic F127 (Poloxamer 407) from BASF (Parsippany, NJ). Solvents such as methanol, 1,4-dioxane, glacial acetic acid and other chemical reagents were of analytical quality.

2.2. Foam preparation

Processing condition 1: PLGA polymer (9% (w/v)) was dissolved in an 87/13 (v/v) mixture of 1,4-dioxane and distilled deionized water by warming at ca. 40°C with magnetic stirring until the polymer solution became clear. This temperature was above the cloud point temperature. The homogeneously clear solution was maintained at 4°C for 0, 2, and 10 min, in order to induce the coarsening effect, before being poured into a disc-shaped brass mold (1 cm in diameter and 5 mm in thickness) which was pre-equilibrated with liquid nitrogen. Solvents were removed by freeze-drying for 3 d.

Processing condition 2: PLLA and PDLLA polymers (12.5% (w/v)) were, respectively, dissolved in an 87/13 (v/v) mixture of dioxane and distilled deionized water by warming at 60°C (above the cloud point) with magnetic stirring. The homogeneously clear solution was maintained at room temperature for 5 min in order to observe the coarsening effect, poured into the aluminum foil mold (disc, 5 cm in diameter and 5 mm in thickness), and then fast-frozen in liquid nitrogen. Solvents were removed by freeze-drying for 3 d.

Processing condition 3: PLLA polymers (10 and 15% (w/v)) were respectively dissolved in an 87/13 (v/v) mixture of dioxane and water by warming at ca. 60°C (above the cloud point) with magnetic stirring. The homogeneously clear solution was air-cooled down until the polymer solution became cloudy and then maintained at ca. 5°C below the cloud point for 1 min. The cloudy polymer solutions were then poured into a disc-shaped brass mold (5 cm in diameter and 5 mm in thickness) pre-equilibrated at dry-ice/ethanol temperature. Solvents were removed by freeze-drying for 3 d.

Processing condition 4: PLGA polymer (6% (w/v)) was dissolved in an 87/13 (v/v) mixture of dioxane/water by magnetic stirring. Three % (w/v) Pluronic F127 was added to the polymer solution with continuous magnetic stirring. In the case of a mixture of dioxane and water, the solution was heated gently to dissolve the polymer completely. The polymer solution was quenched by liquid nitrogen and then freeze-dried for several days. Freeze-dried sample was placed in pure excess methanol at 4°C for 1 d in order to extract the Pluronic F127. Afterwards, the sample was freeze-dried again for several days.

Processing condition 5: PLGA polymer solutions (4, 6, and 9% (w/v)) in dioxane were prepared by magnetic stirring at ca. 30°C. The homogeneous polymer solution was poured into a brass mold pre-equilibrated with liquid nitrogen temperature. Solvents were removed by freeze-drying for 3 d. The sample was then freeze-dried again for 3 d.

2.3. Scanning electron microscopy (SEM)

Scanning electron microscopy (SEM, Philips 535M) was used for the observation of the internal pore morphology of the freeze-dried foams. The samples were fractured by a surgical blade and then coated with gold by using a sputter-coater (HUMMER V, Technics, USA). Ar gas pressure was set at 5 psi and the current was maintained at 10 mA for a coating time of 5 min.

2.4. Mercury intrusion porosimetry

Mercury intrusion porosimetry (PMI 30K-A-1, Porous Materials, Inc., Ithaca, NY) was used to determine pore size distribution, total pore volume, and surface area of the foams. Pore size and surface area were calculated from the measurement of the intruded mercury volume by raising pressure [20].

2.5. Protein loading and distribution analysis

Ten % (w/v) PLLA polymer foams prepared by processing condition 3 were cut in a dimension of 7 mm × 7 mm × 3.6 mm. They were pre-wetted in pure ethanol at 4°C for 14 h under static condition and ethanol was then replaced by excess water with orbital shaking [21]. Carbonic anhydrase II was loaded into the pre-wetted foams by dipping them into the protein solution (4.44 mg/ml) at room temperature for 38 h. Loading quantity was determined by measuring the remaining amount of protein in the solution. In order to analyze the distribution of the protein incorporated into the foams, the protein-loaded foams were dipped into a Coomassie Blue solution, which consisted of 0.1% (w/v) Coomassie Blue R-250, 45% (v/v) methanol, 45% (v/v) water, and 10% (v/v) glacial acetic acid. After incubation for several hours, the dye was destained by using a solution of 10% (v/v) methanol, 10% (v/v) glacial acetic acid, and 80% (v/v) water. The dye penetrating depth was then determined.

3. Results and discussion

Cloud points for different concentrations of PLLA, PDLLA, and PLGA in a mixture of dioxane and water with 87/13 volume ratio were previously determined by the visual inspection of polymer solution clarity [19]. It should be mentioned that the constructed cloud point curves would not coincide with the binodal curve, since polydisperse polymers were used in our experiment. Thus, phase diagram could not be constructed based on the observed cloud points. However, it is believed that the determination of cloud points could be utilized as a good criterion dividing the homogeneous and the phase separated region [17].

Fig. 2 shows amorphous PLGA microcellular foams obtained by coarsening 9% (w/v) polymer solution at

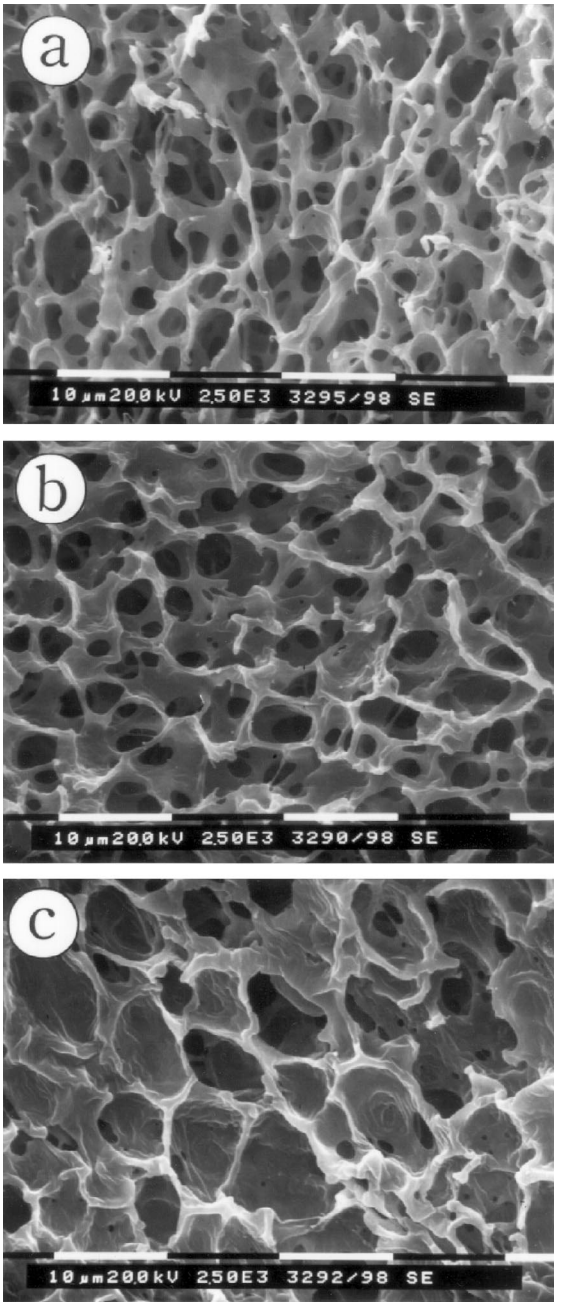

Fig. 2. SEM images of the cross section of amorphous PLGA foams as a function of coarsening time. The foams were prepared by coarsening 9% (w/v) polymer solution at 4°C for 0 min (a), 2 min (b), 10 min (c), and then quenching by liquid nitrogen.

4°C for different time intervals of 0, 2, and 10 min and subsequent quenching into liquid nitrogen (processing condition 1). The cloud point of 9% (w/v) PLGA polymer solution was about 20°C in an 87/13 (v/v) mixture of dioxane and water. The morphologies were open cellular microporous structure with average pore sizes ranging 1–10 μm, suggesting that a spinodal decomposition mechanism was responsible for these structures as similarly reported elsewhere [18]. The SEM observation evidently shows the effect of the coarsening time on the resultant foam morphology. As the coarsening time was extended, the pore size increased and bi-continuous open structure tended to become more closed cellular structure. This agrees well with the general trend of the coarsening effect found in the other polymer membranes [18,22].

PLLA and PDLLA foams prepared by using 12.5% (w/v) polymer solution with different phase-separation conditions (processing condition 2) are demonstrated in Fig. 3. For the PLLA foam, the resultant pore morphologies were compared under two different conditions: (i) direct quenching into liquid nitrogen and (ii) allowing 5 min coarsening time at room temperature prior to immersion into liquid nitrogen. Greater enlargement of pore size can be seen with permitting the coarsening process, as expected. The PDLLA foam was prepared under the same coarsening condition to the PLLA foam. It shows the combined presence of large pores and many small pores with a tendency of stringy/beady morphology in contrast to the PLLA foam. At 12.5% (w/v) polymer concentration, the cloud points of PLLA and PDLLA were 41 and 27°C, respectively [19]. Thus, the PDLLA foam produced by coarsening at room temperature just below the cloud temperature was likely to first undergo a nucleation and growth mechanism in the metastable region as a prerequisite step directing towards the spinodal decomposition occurring in the unstable region. This might result in different morphologies in the PDLLA foam compared to the PLLA foam. Additionally, PLLA, which is semi-crystalline in nature in contrast to amorphous PDLLA, might crystallize after the liquid–liquid demixing and resulted in the different foam morphology [23].

PLLA foams from 10 and 15% (w/v) polymer solution were prepared by a two-step quenching process: first, slow cooling down to 5°C lower than the cloud temperature (41 and 43°C for 10 and 15% (w/v) PLLA concentration, respectively) and maintaining for 1 min at that temperature, and as a second step, rapid quenching in a brass mold pre-equilibrated with liquid nitrogen. The resultant foam morphologies are represented in Fig. 4 (processing condition 3). Distinctive multi-modal distribution of pores composed of large pores up to 100 μm and many micropores are clearly observed in both cases, although 15% sample has more well-defined round shaped pores. This interesting morphology has been

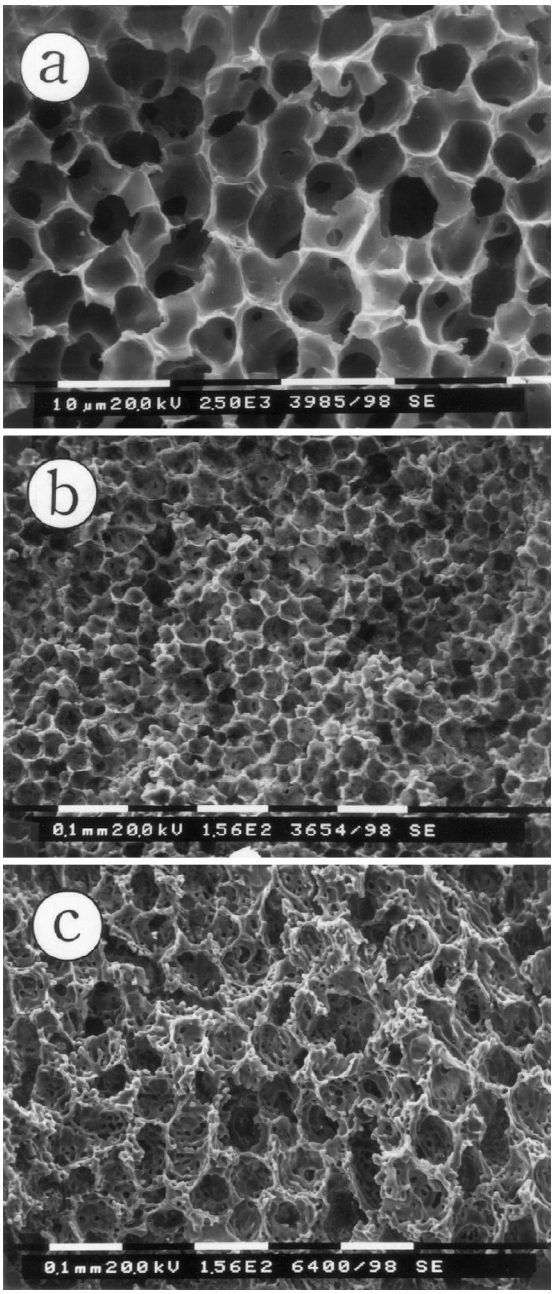

Fig. 3. SEM images of the cross section of 12.5% (w/v) semi-crystalline PLLA and amorphous PDLLA foams. (a) PLLA, direct liquid nitrogen quenching; (b) PLLA, 5 min coarsening at room temperature; (c) PDLLA, 5 min coarsening at room temperature

reported in other polymer–solvent systems [18]. This phenomenon can be attributed to the two-step-phase separation: (i) gradual-phase separation during the slow cooling process and (ii) spinodal decomposition during faster cooling process. The large pores were presumed to preferentially generate during the first step, since the kinetic time scale of the second step for arresting the phase separation was too short. The morphological difference between the 10 and 15% PLLA foams can be

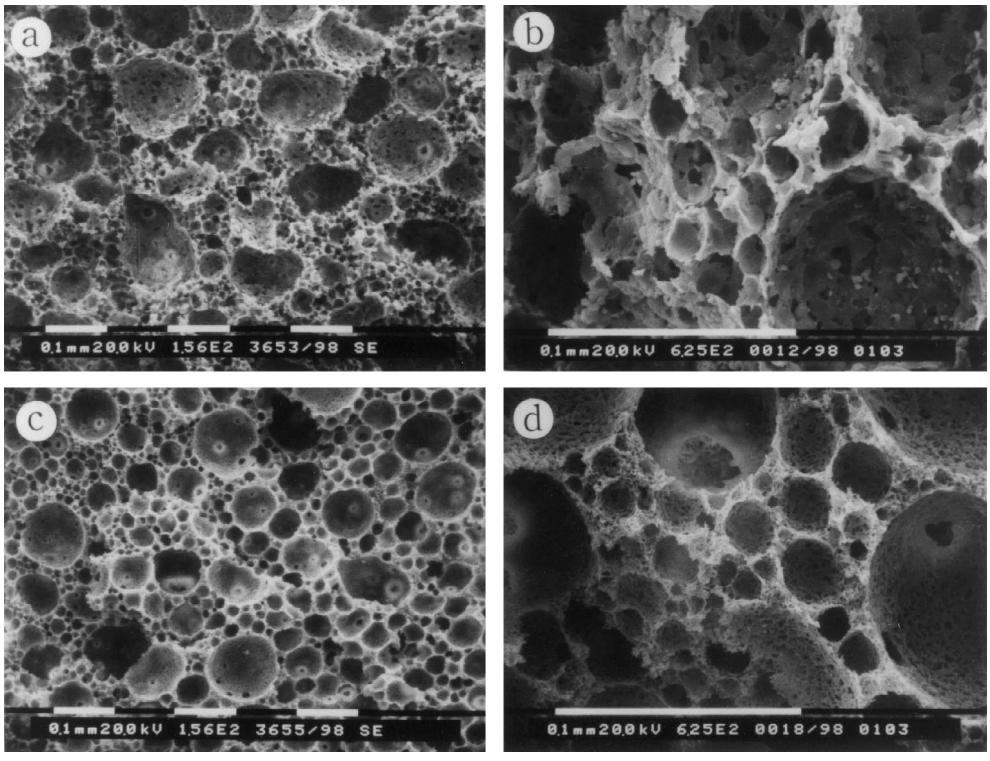

Fig. 4. SEM images of the cross section of 10 and 15% (w/v) PLLA foams. They were prepared by cooling down the polymer solution to 5°C below the cloud point, maintaining for 1 min, and then quenching by liquid nitrogen. 10% (w/v) PLLA (a), (b); 15% (w/v) PLLA (c), (d).

explained by different quenching routes. Since the selected quenching routes in this experiment were located in the left side of the critical polymer concentration, 10% polymer solution had more probability to be located within the deeper metastable region than 15% polymer solution. This means that the nucleation and growth process can get involved in the early stage phase separation to a greater extent. Therefore, characteristic morphology of the 10% PLLA foams, which is different from the well-defined round-shaped pore structure of the 15% sample, was caused by more involved nucleation and growth mechanism of polymer-rich phase. Many micropores are also observed between the isolated macropores, which might be generated, upon further quenching in dry-ice/ethanol, from spinodal decomposition in the excluded polymer-rich phase formed in the first-step process, as reported [18].

Selected PLGA, PDLLA, and PLLA foams were characterized in terms of total pore volume, surface area, and porosity by a mercury intrusion porosimetry. The results are listed in Table 1. Fig. 5 shows pore size distributions of the selected foams. The PLGA foam prepared with 9% (w/v) polymer concentration and 10 min coarsening time exhibits microporous structure having a mean pore diameter of 8.5 μm, as observed in the SEM picture in Fig. 2c. The PDLLA foam prepared with 12.5% (w/v) polymer solution shows multi-modal distribution of pore

Table 1
Characterization of porous polymer foams by mercury intrusion porosimetry

	Intrusion volume (ml/g)	Surface area (m^2/g)	Porosity
9% PLGA	5.00	2.77	0.89
12.5% PDLLA	6.74	0.89	0.92
10% PLLA	5.03	2.27	0.85
15% PLLA	3.37	5.88	0.76

diameters with appearing two major peaks centered at 6.9 and 28 μm. The two PLLA foams prepared by the two step quenching process; they show small pores ranging 1–2 μm and micropores ranging 8–18 μm as observed in the SEM picture in Fig. 4. However, large macropores near 100 μm which are clearly found in the SEM picture could not be detected in the result of mercury porosimetry, perhaps due to the limitation of mercury intrusion method [7,20]. For the detection of large pores by a mercury intrusion technique, the facile penetration of pressurized mercury through tortuous interconnected channels of surrounding small pores should occur to access the large pores. Even high pressure was applied to intrude mercury into the polymer foams, the accessibility of mercury to the large pores would be

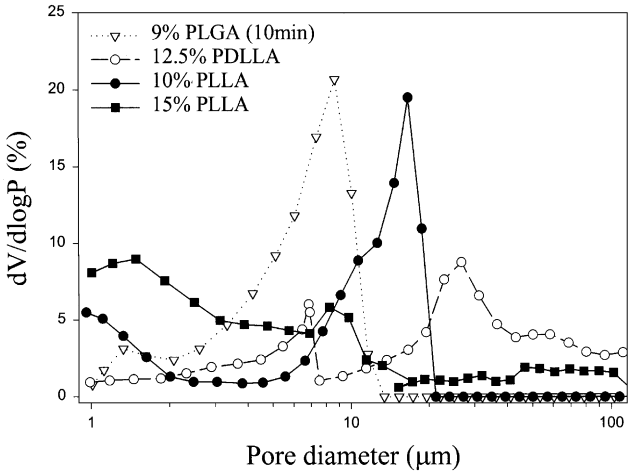

Fig. 5. Pore size distribution of the selected foams determined by mercury intrusion porosimetry.

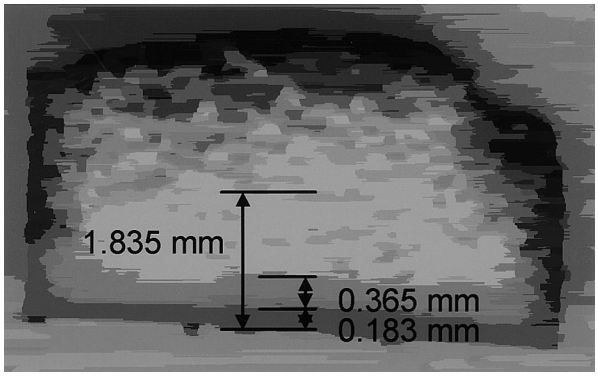

Fig. 6. Cross-sectional image of Coomassie Blue stained-protein distribution in the 10% (w/v) PLLA foam.

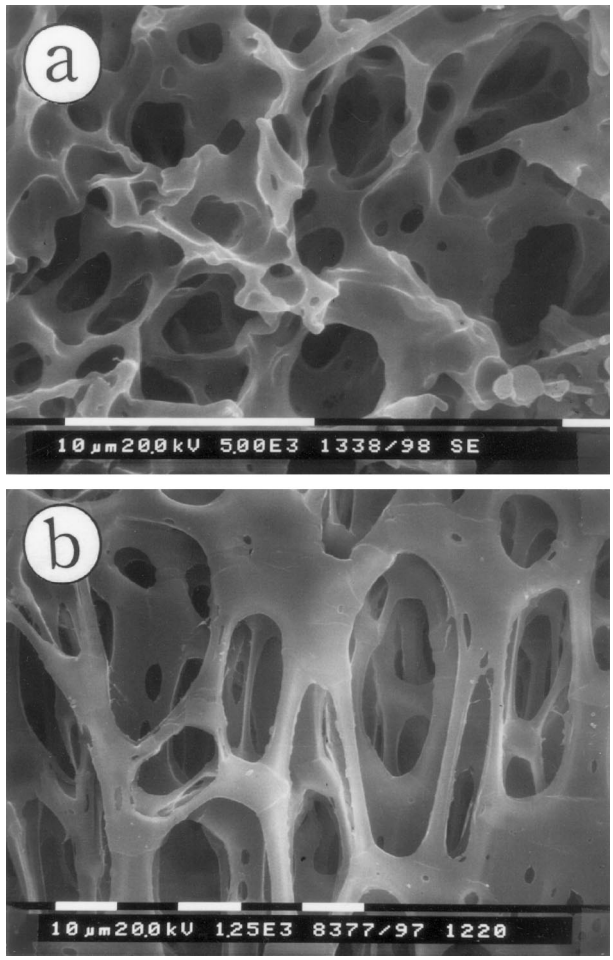

Fig. 7. SEM images of the cross section of PLGA foams. The foams were prepared by quenching 6% (w/v) PLGA solution without (a) or with (b) 3% (w/v) Pluronic F127 into liquid nitrogen.

limited due to their isolated distribution. This is the most plausible reason for not detecting the large macropores in the mercury intrusion method in contrast to the SEM observation. This problem is particularly acute for the foams having broad pore size distribution with a closed cellular structure.

The 10% (w/v) PLLA polymer foam prepared by the two-step quenching method was used for protein distribution study. A model protein, carbonic anhydrase (MW 31 000) was loaded into the foam by an immersion-soaking method. Fig. 6 shows protein specific staining extent of Coomassie Blue dye for the cross-sectional area of the foam, which exhibits spatial distribution of protein loaded within the foam matrix. The protein molecules were located in the peripheral region, indicating that the foam was not well inter-connected or the wall of small pores was not completely wetted in spite of the ethanol pre-wetting treatment. This protein staining result corresponds to the aforementioned limitation of mercury intrusion method for detecting the closed large pores in the foam matrix.

It is of interest to add an additive in the TIPS formulation to modify the pore geometry and size [24]. As reported previously, the final morphology of the foams is determined by a kinetically arrested state of the phase separating system [19]. Since TIPS process produces two-phase-separated domains having different interfacial energies at their surface, tri-block copolymer surfactant composed of poly(ethyleneglycol)–poly(propyleneglycol)–poly(ethyleneglycol), Pluronic F127, was added to examine its interface compatibilization effect on the foam morphology. Fig. 7 demonstrates the SEM picture of 6% (w/v) PLGA foam prepared by using an 87/13 dioxane/water mixture with and without adding 3% (w/v) Pluronic F127 (processing condition 4). The Pluronic surfactant was later removed by incubating the freeze-dried foam in a methanol solution. It can be seen that the addition of Pluronic surfactant effectively produced more enlarged open cellular pores up to 50 μm while concomitantly maintaining more round pore shapes. This suggests that Pluronic surfactant indeed reduced the interfacial energy between phase-separated

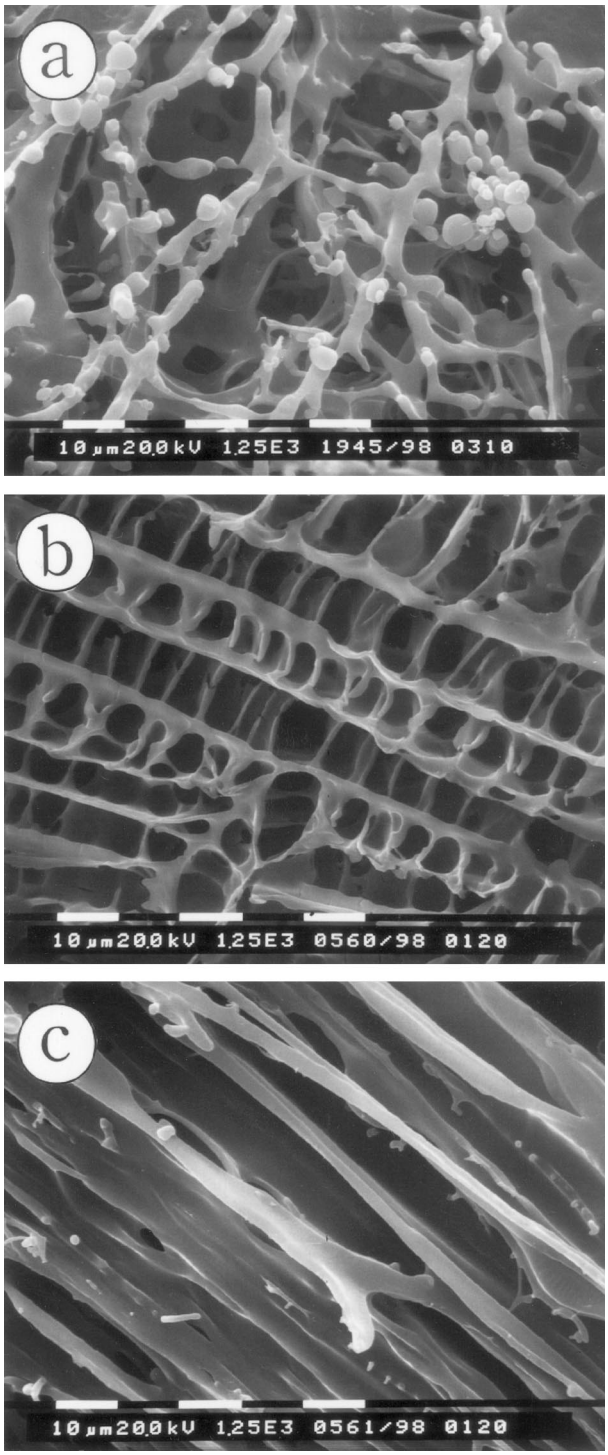

Fig. 8. SEM images of the cross section of PLGA foams produced by quenching 4% (a), 6% (b), 9% (c) (w/v) polymer solution in pure dioxane into liquid nitrogen.

polymer-rich phase and polymer-poor phase in the spinodal decomposition by acting as a phase compatibilizer. The foam obtained by adding Pluronic surfactant appears to be suitable for seeding of appropriate cells due to its pore size and geometry.

Finally, the use of pure dioxane as a sole solvent, instead of dioxane/water mixture, for a solid–liquid TIPS process was tried to fabricate PLGA foams. Various concentrations of PLGA dissolved in dioxane were rapidly quenched into liquid nitrogen. Fig. 8 shows the SEM pictures of PLGA foams obtained. With increasing the polymer concentration in the order of 4, 6, and 9% (w/v), the morphology changes beady/stringy, ladder-like, and tube-like structure, respectively (processing condition 5). In the case of 6% (w/v) polymer solution, a similar morphology was recently reported [6]. These anisotropic morphologies were likely to be developed by a solid–liquid-phase separation, in which preferential crystallization of pure dioxane dominantly occurred in the direction of heat transfer. The formation of a beady/stringy structure at 4% (w/v) polymer concentration suggests that the nucleation and growth mechanism proceeded at this polymer concentration as a major TIPS pathway.

4. Conclusions

It has been shown that various microcellular and porous foam morphologies could be obtained by adjusting the TIPS parameters. A slight change in the parameters, such as types of polymer, polymer concentration, solvent/nonsolvent ratio, and the most importantly, thermal quenching strategy, significantly affected the resultant foam morphology. In particular, the addition of polymeric surfactant in the TIPS formulation enhanced the size of pores and improved their inter-connectivity. The prepared foams could find applications in controlled drug delivery.

Acknowledgements

This work was supported in part from the Biotechnology-2000 Program (Grant #97-N1-02-05-A-04) by the Ministry of Science and Technology, South Korea.

References

[1] Freed L, Marquis JC, Nohria A, Emmanual J, Mikos AG. Neocartilage formation in vitro and in vivo using cells cultured on synthetic biodegradable polymers. J Biomed Mater Res 1993;27:11–23.

[2] Mikos AG, Bao Y, Cima LG, Ingber DE, Vacanti JP, Langer R. Preparation of poly(glycolic acid) bonded fiber structures for cell attachment and transplantation. J Biomed Mater Res 1993;27:183–9.

[3] Mikos AG, Sarakinos G, Leite SM, Vacanti JP, Langer R. Laminated three-dimensional biodegradable foams for use in tissue engineering. Biomaterials 1993;14(5):323–30.

[4] Mikos AG, Thorsen AJ, Czerwonka LA, Bao Y, Langer R, Winslow DN, Vacanti JP. Preparation and characterization of poly(L-lactic acid) foams. Polymer 1994;35(5):1068–77.

[5] Lo H, Kadiyala S, Guggino SE, Leong KW. Poly(L-lactic acid) foams with cell seeding and controlled-release capacity. J Biomed Mater Res 1996;30:475–84.
[6] Schugens Ch, Maguet V, Grandfils Ch, Jerome R, Teyssie Ph. Polylactide macroporous biodegradable implants for cell transplantation. 2. Preparation of polylactide foams by liquid–liquid phase separation. J Biomed Mater Res 1996;30:449–61.
[7] Whang K, Thomas CH, Healy KE, Nuber G. A Novel methods to fabricate bioabsorbable scaffolds. Polymer 1995;36(4):837–42.
[8] Mooney DJ, Baldwin DF, Suh NP, Vacanti JP, Langer R. Novel approach to fabricate porous sponges of Poly(D,L-lactic-co-glycolic acid) without the use of organic solvents. Biomaterials 1996;17:1417–22.
[9] Harris LD, Kim BS, Mooney DJ. Open pore biodegradable matrices formed with gas foaming. J Biomed Mater Res 1998; 42:396–402.
[10] Aubert JH, Clough RL. Low density, microcellular polystyrene foams. Polymer 1985;26:2047–54.
[11] Lloyd DR, Kinzer KE, Tseng HS. Microporous membrane formation via thermally induced phase separation. I. Solid–liquid phase separation. J Membr Sci 1990;52:239–61.
[12] Lloyd DR, Kim SS, Kinzer KE. Microporous membrane formation via thermally induced phase separation. II. Liquid–liquid phase separation. J Membr Sci 1991;64:1–11.
[13] van de Witte P, Dijkstra PJ, van den Berg JWA, Feijen J. Phase separation processes in polymer solutions in relation to membrane formation. J Membr Sci 1996;117:1–31.
[14] Mulder M. Preparation of synthetic membranes. In: Basic principles of membrane technology. Dordrecht, Netherlands: Kluwer Academic Publishers, 1996. p. 71–156.
[15] Bansil R, Liao G. Kinetics of spinodal decomposition in homopolymer solutions and gels. Trends Polym Sci 1997;5(5):146–54.
[16] Siggia ED. Late stage of spinodal decomposition in binary mixtures. Phy Rev A 1979;20:595.
[17] Tsai FJ, Torkelson JM. Roles of phase separation mechanism and coarsening in the formation of poly(methyl methacrylate) asymmetric membranes. Macromolecules 1990;23:775–84.
[18] Song SW, Torkelson JM. Coarsening effects on the formation of microporous membranes produced via thermally induced phase separation of polystyrene–cyclohexanol solutions. J Membr Sci 1995;98:209–22.
[19] Nam YS, Park TG. Porous biodegradable polymeric scaffolds prepared by thermally induced phase separation. J Biomed Mater Res 1999; in press.
[20] Ritter HL, Drake LC. Pore-size distribution in porous materials. 1. Pressure porosimeter and determination of complete macropore-size distribution. Ind Engng Chem 1945;17:782–6.
[21] Mikos AG, Lyman MD, Freed LE, Langer R. Wetting of poly(L-lactic acid)and poly(D,L-lactic-co-glycolic acid) foams for tissue culture. Biomaterials 1994;15(1):55–8.
[22] Guo HF, Laxminarayan A, Cabeba GT, Solc K. Morphological studies of late-stage spinodal decomposition in polystyrene–cyclohexanol system. J Appl Polym Sci 1995;55:753–9.
[23] van de Witte P, Boorsma A, Esselbrugge H, Dijkstra PJ, van den Berg JWA, Feijen J. Differential scanning calorimetry study of phase transitions in poly(lactide)-chloroform-methanol systems. Macromolecules 1996;29:212–9.
[24] Cha BJ, Char L, Kim JJ, Kim SS, Kim CK. The effect of diluent molecular weight on the structure of thermally induced phase separation membrane. J Membr Sci 1995;108:219–29.